

242

[REDACTED]

LIBRARY
TECHNICAL REPORT SECTION
NAVAL POSTGRADUATE SCHOOL
MONTEREY, CALIFORNIA 93940

Technical Report No. 36

SACLANT ASW
RESEARCH CENTRE

EM PHENOMENA IN THE ELF RANGE:
EM FIELDS OF SUBMERGED DIPOLES AND FINITE ANTENNAS

by

L. BROCK-NANNESTAD

1 JUNE 1965

[REDACTED]

VIALE SAN BARTOLOMEO, 92
LA SPEZIA, ITALY

[REDACTED]

AD 0466137

~~NATO UNCLASSIFIED~~

TECHNICAL REPORT NO. 36

SACLANT ASW RESEARCH CENTRE

Viale San Bartolomeo 92

La Spezia, Italy

EM PHENOMENA IN THE ELF RANGE:

EM FIELDS OF SUBMERGED DIPOLES AND FINITE ANTENNAS

By

L. Brock-Nannestad

APPROVED FOR DISTRIBUTION



HENRIK NODTVEDT

Director

~~NATO UNCLASSIFIED~~

TABLE OF CONTENTS

	<u>Page</u>
PREFACE TO THE SERIES	1
ABSTRACT	4
LIST OF SYMBOLS AND ABBREVIATIONS	5
INTRODUCTION	7
1. THE EM FIELD FROM DIPOLES	9
1.1 Sinusoidal Excitation	9
1.2 Corrections for Discontinuities	17
1.3 Transient Excitation	21
2. THE EM FIELD FROM FINITE ANTENNAS	24
3. ESTIMATE OF THE ACCURACY OF FIELD-STRENGTH CALCULATIONS AND MEASUREMENTS	27
4. EXPERIMENTS CONCERNING EM-FIELDS AND PROPAGATION	28
REFERENCES	31
FIGURES	
1. Skin depth as a function of the relevant frequencies for various conductivity values typical of sea-water	32
2. Expressions for the field-strength of horizontal dipoles	33
3. Expressions for the field-strength of vertical dipoles	34
4. Geometry of the measurements of horizontal field strength	35
5. Modulus of the transfer function E_x / M as a function of x_1 and with θ as a parameter	36

TABLE OF CONTENTS (Continued)

	<u>Page</u>
6. The angle dependence of the horizontal E components at the surface and where $ \gamma\rho \gg 1$	37
7. The influence of the sea-bed on propagation	38
8. Correction factor for use with limited water-depths	39
9. Model of an insulating island in an ocean	39
10. West-east cross section of the island of Tino	40
11. Values of H_x/H_o and E_z/E_o at various points on the model of Tino	40
12. Calculation of the field from a coaxial antenna in a conducting medium	41
13. Estimate of errors in field expressions for $E_{1\rho}$ of dipoles at the boundary	42
14. Estimate of errors in field expressions for $E_{1\varphi}$ of dipoles at the boundary	43
15. Waveform of transmitter current	44
16. Result of propagation experiment	45
APPENDIX I	46

EM PHENOMENA IN THE ELF RANGE

By

L. Brock-Nannestad

PREFACE TO THE SERIES

The series of three reports published under the general heading of "Electromagnetic Phenomena in the Extremely Low Frequency Range" provides a final summary of the research in this field carried out by the SACLANT ASW Research Centre between the end of 1959 and the end of 1964.

The reports are based mainly on a number of Technical Notes distributed only within the Centre itself. Short reports of current work have appeared regularly in the Centre's Quarterly Status Reports and, on occasions, in briefing material for various Scientific Committees. However, the present series is the first comprehensive description of the research carried out in this field by the Centre.

Naturally, as in all scientific work, some work that was started turned out to be less fruitful than expected. In addition, the departure of scientists studying particular fields has brought those aspects of the work to an end. For example, work on a magnetometer based on nuclear magnetic resonance, which had shown some promise, had to be discontinued for this latter reason. In order to maintain continuity, a number of such inconclusive or uncompleted studies are omitted from these reports.

The size of the Electromagnetic Research Group did not permit a broad attack on all the problems involved, and, after an initial research period, the effort was concentrated on a few aspects. For this final summary these have been divided

into three groups — each reported separately.

The first report deals mainly with EM fields of submerged dipoles and finite antennas. A large amount of work in this field has been done by other investigators, and some of the results of this work have been used in this theoretical study. The second report deals with the EM background noise in the ELF range and the instrumentation developed for its measurement, which constituted the main part of the Centre's work on EM phenomena in the ELF range. The third report, which is classified, deals with the special applications to ASW.

The major part of the research was carried out during a period when similar work was being done in many other places. The number of published papers on the subject has increased rapidly, doubling within only the last three years. To keep track of these developments, a bibliography was prepared in 1962. Since then, the rapid increase has demanded a second edition (Ref. 1), which was published in 1964. As practically all phenomena in the ELF range are related in one way or another to phenomena outside this range, the bibliography also includes papers on geomagnetic disturbances below 1 cps and VLF phenomena above 3,000 cps. It thus contains abstracts of about 1,700 papers and is used as a general reference throughout this series. In specific cases, however, direct reference is made to the individual papers listed in each report's bibliography.

During the research period, the following scientists (listed alphabetically) have worked for longer or shorter periods in the Group.

L. Brock-Nannestad (Denmark)

Y. Faroudja (France)

K. Hansen (Denmark)

J. Marthins (Norway)

P. E. Mijnaerends (Netherlands)

H. Rynja (Netherlands)

E. Sirovich (Italy)

T. Strarup (Denmark)

G. Tacconi (Italy)

The present series contains contributions from all the above, but, for clarity, the individual contributions are not presented separately and references are only made when the work has been reported in the open literature. The series of reports thus represents the work of the whole group.

The author, who has been Group Leader throughout, wishes to acknowledge the collaboration and contributions of his colleagues in this research. The main part of the work was carried out during a period in which the Centre was under the directorship of Dr. E. T. Booth and Dr. J. M. Ide, and the author expresses his thanks to them for their interest and support.

THE ELECTROMAGNETIC FIELD FROM SUBMERGED DIPOLES
AND
FINITE ANTENNAS

ABSTRACT

The report is the first of a series of three that discusses various EM phenomena in the ELF range.

The expressions for the various components of the EM field from submerged dipoles are presented. Although similar expressions can be found in the published literature, one of the purposes of this report is to present them together using the same notations and measuring units.

Applications of the theories to special situations such as discontinuities, transients and finite antennas are described and the accuracy of field expressions is determined. Some propagation experiments are briefly mentioned.

LIST OF SYMBOLS AND ABBREVIATIONS

A	=	complex transmission factor
A'	=	correction factor
amp-m	=	ampere metre
amp/m	=	amperes per metre
d	=	water-depth
δ	=	skin-depth
$E, "E"$	=	electric field-strength; subscript indicates the particular component, (vpm).
ELF	=	extremely low frequencies, (1-3000 cps).
ϵ_0	=	free space dielectric constant
ϵ_1	=	dielectric constant of conducting medium
$F, "F"$	=	transfer functions
f	=	frequency, (cps).
γ_0	=	intrinsic propagation constant, air
γ_1, γ	=	" " " , conducting medium
γ_2	=	" " " , sea bed
H	=	magnetic field-strength; subscript indicates the particular component, (amp/m).
h	=	depth of transmitter
I, I_0	=	current , (amp)
ℓ	=	length of insulated wire
L	=	length of bare wire
λ_0	=	free-space wave-length
λ_1	=	wave-length in conducting medium
M	=	dipole moment, (amp-m)
m	=	metre
mho	=	unit of conductivity

μ_0	=	free space permeability
ω	=	angular frequency
Π	=	Herz potential
R, R'	=	distance between antenna and point of observation
r	=	characteristic variable in A
r_0	=	radius of insulating platform
ρ	=	horizontal separation between transmitter and receiver
σ, σ_1	=	conductivity of lossy medium
t	=	time
vpm	=	volts per metre
z'	=	co-ordinate along antenna
(x, y, z)	=	cartesian coordinates
(ρ, φ, z)	=	cylindrical coordinates
(ξ, η)	=	elliptical coordinates
$(\theta, \alpha, \rho_0, x_1)$	=	parameters describing relative position of transmitter and receiver.

INTRODUCTION

A large number of scientists have investigated the fields generated by dipoles embedded in a lossy medium. The present author's "Bibliography of EM Phenomena" (Ref. 1) contains 250 references on this subject. Most of the published papers are theoretical, with more or less elegant solutions of the mathematical problems involved. However, a number of papers describe experiments that confirm the basic propagation laws. This present report leans heavily on the work of a number of scientists, among whom J.R. Wait has been the most productive. In addition, during the earlier part of the research, the much-cited work of Banos and Wesley (Ref. 2) was used as a basis of calculation.

Even if the basic laws for the generation of fields and for their propagation seem to be well established, there remain specific problems. In the bulk of the theoretical papers the calculations have been simplified by assuming idealised conditions, such as a semi-infinite conducting medium. The problem of deviations from this ideal situation has been approached, for example, by Wait in his treatment of the coastline effects caused by more or less rapid conductivity changes in the horizontal plane.

It is also a general feature of most of the published papers that the results are presented in terms of non-dimensional parameters, and that the mathematical operations are subject to approximations that can restrict the validity of the expression. This can result in confusion when comparing different papers.

In this present report only the very near fields of dipoles are considered. In these cases, the range — the distance between dipole and point of observation — is always very much smaller than the wavelength in air, but it can vary from

zero to several times the wavelength in the conducting medium. Within such a range the influence of the ionosphere on the fields is generally neglected, and it is also assumed that the static magnetic field of the earth has no influence on the fields. In general, the conducting medium is assumed to be seawater, which has a conductivity of 4 mho/m.

At the end of the report a few experiments are mentioned. These were carried out to gain familiarity with the whole technique, rather than to prove or disprove a theoretical result. Model experiments, using small volumes of mercury and high frequencies instead of large volumes of water and ELF, have been suggested as substitutes for large-scale experiments. This technique was tried in an attempt to determine experimentally the distribution of the currents around an antenna several skin-depths long and at various distances from the boundary. However, there were considerable experimental difficulties and the results were unreliable.

The effect of reflections from the boundaries of the tank make model experiments less attractive than they appear on paper, unless a large effort in lay-out and equipment is made. Similarly, full scale experiments are subject to the influence of boundaries such as coastlines. During the earlier part of the research programme these effects introduced confusing errors in the measurements, and some effort was spent determining the sources of error. A few details about this part of the work are given.

In this report emphasis will be put on presenting the formulas and expressions needed for the calculation of those components of the EM field that were of major interest to the whole project. As shown in the second report (T. R. 37) of this series, the horizontal electric-dipole is theoretically the most efficient receiver for EM energy in the ELF range when working from a floating platform, and for this reason theoretical work was also concentrated on the horizontal electric-dipole and the field generated by it.

1. THE EM FIELD FROM DIPOLES

Many authors have dealt with the problem of calculating the EM fields from dipoles. Probably Sommerfeld (Ref. 3) was the first to give the formal solution. Based on this work, Wait (Ref. 4) gave self-contained derivations for the special cases that arise. The following résumé will be based mainly on this latter work.

The field from dipoles is generally divided into three overlapping distance ranges that relate the horizontal separation, ρ , between transmitter and receiver to the free-space wavelength, λ_0 :

Case I, $\rho \gg \lambda_0$, is the "radiation field",

Case II, $\rho \sim \lambda_0$, is the "near field", and

Case III, $\rho \ll \lambda_0$, is called the "quasistatic case".

In the present research on EM phenomena the last case is the most important because the free-space wavelengths in the ELF range are extremely large. The solutions in Case III are also dependent on the relation between the horizontal separation, ρ , and the wavelength in the conducting medium, λ_1 . This relation has been treated in detail by Wait (Ref. 4). The derivations will not be repeated here; only the final results and the ranges within which they are valid will be presented.

1.1 Sinusoidal Excitation

In field problems of this kind it is customary to let the conducting medium occupy the half-space $z \geq 0$ with reference to a Cartesian coordinate system (x, y, z) . The electric dipole of infinitesimal length $d\ell$ is oriented along the x-axis and situated at $(0, 0, h)$.

The intrinsic propagation constant of the upper medium, air, is defined as:

$$\gamma_0^2 = -\epsilon_0 \mu_0 \omega^2 \quad (\text{Eq. 1})$$

that of the conducting medium as:

$$\gamma_1^2 = i\sigma_1 \mu_0 \omega - \epsilon_1 \mu_0 \omega^2 \quad (\text{Eq. 2})$$

where ϵ_0 and μ_0 are the free space dielectric constant and the free space permeability, respectively, and where ϵ_1 and σ_1 are the conducting medium dielectric constant and the conducting medium conductivity, respectively.

In the frequency range of interest, the first term in Eq. 2 is much larger than the second term; therefore, throughout this section, the second term will be neglected. In other words, this means that the conduction current is considered much larger than the displacement current in the conducting medium. Eq. 2 then reduces to:

$$\begin{aligned} \gamma_1 &= \sqrt{i\mu_0 \omega \sigma_1} \\ &= \frac{1+i}{\delta} \\ &= \frac{\sqrt{2}}{\delta} e^{i\frac{\pi}{4}} \end{aligned} \quad (\text{Eq. 3})$$

where δ is the skin-depth in the conducting medium at the angular frequency $\omega = 2\pi f$. Fig. 1 represents the skin-depth as a function of the relevant frequencies for various conductivity values typical of seawater. It is further

assumed that

$$|\gamma_1| \gg |\gamma_0|$$

which will be true in the case of seawater.

For the range of horizontal distance, ρ , in which simultaneously $|\gamma_0 \rho| \ll 1$ and $|\gamma_1 \rho| \gg 1$, the expressions for the field-strength of the various components of the horizontal electric-dipole are as given in Fig. 2. This situation is generally considered to be the most important, but it is interesting to compare these expressions with the corresponding expressions for a horizontal magnetic-dipole, given on the same figure. Similarly, for the sake of completeness, Fig. 3 gives the expressions for both vertical electric and vertical magnetic dipoles.

In all expressions, the subscript 1 has been omitted from both the propagation constant and the conductivity symbols. Thus $\gamma = \gamma_1$ and $\sigma = \sigma_1$. The source strength of the dipole is expressed as the dipole moment M , which is defined as:

$$M = I \cdot d\ell$$

for the electric dipole, and as

$$M = I \cdot dA$$

for the magnetic dipole, where dA represents an infinitesimal area. Time enters according to the factor $\exp(i \omega t)$, but this has been left out in the present part of this report.

The expressions for the field of the horizontal electric-dipole become more complicated when the condition $|\gamma\rho| = |\gamma_1\rho| \gg 1$ is not fulfilled. In this case only the components E_ρ , E_φ and H_z can be written in concise form. According to Wait (Ref. 4):

$$E_\rho = \frac{M}{2\pi\sigma} \cdot \frac{1}{\rho^3} \left[1 + (1 + \gamma\rho) e^{-\gamma\rho} \right] \cos \varphi \quad (\text{Eq. 4})$$

$$E_\varphi = \frac{M}{2\pi\sigma} \cdot \frac{1}{\rho^3} \left[2 - (1 + \gamma\rho) e^{-\gamma\rho} \right] \sin \varphi \quad (\text{Eq. 5})$$

$$H_z = \frac{M}{2\pi\gamma^2} \cdot \frac{1}{\rho^4} \left[3 - (3 + \gamma\rho + \gamma^2\rho^2) e^{-\gamma\rho} \right] \sin \varphi \quad (\text{Eq. 6})$$

These equations are valid for $h = z = 0$ and $|\gamma_0\rho| \ll 1$. The value of $|\gamma\rho|$ is, however, unrestricted. For $|\gamma\rho| \gg 1$ the expressions agree with those given in Fig. 2, and when $|\gamma\rho|$ approaches zero they reduce to forms consistent with potential theory. The fields do not, in this case, vary in a simple manner with z and h . Nor does the exponential attenuation with depth — which was present in the expressions for $|\gamma\rho| \gg 1$ — apply to Eqs. 4, 5 and 6. Wait (Ref. 4) presents expressions for the fields in terms of modified Bessel functions for the case where $z > 0$ and $h > 0$.

An attempt has been made to verify Eqs. 4 and 5 experimentally and to determine the depth dependence. In a full scale experiment one dipole is used as the transmitter, and an electrode system — of the type described in the second report (T.R. 37) of this series — is used to measure the horizontal field close to the surface. During work at sea it can be difficult to maintain the proper orientation for the measurement of E_ρ or E_φ . To suit these particular conditions, Eqs. 4 and 5 have been modified in the following way.

Fig. 4 shows the geometry as seen from above the surface. The transmitting dipole is placed at the origin of the x, y co-ordinates. The field-strength is measured along an arbitrary axis x_1 , that makes the angle θ with the x -axis. For the purpose of calculation it is assumed that the transmitter is fixed and that the receiver moves along the x_1 axis. (During experiments it was found better to keep the receiver fixed and to move the transmitter along the x_1 axis, but this does not change the calculations.)

The various distances and angles needed for the calculation are shown in Fig. 4, and the relationships between some of them are given below. The zero point of the x_1 axis is placed where the transmitter and receiver are closest, the distance between them being ρ_0 . With the symbols used in Fig. 4 one has:

$$\begin{aligned}\rho &= \sqrt{\rho_0^2 + x_1^2} \\ \theta &= \varphi_0 - \frac{\pi}{2} \\ \varphi &= \varphi_0 - \arctan \frac{x_1}{\rho_0} = \theta + \frac{\pi}{2} - \arctan \frac{x_1}{\rho_0} \\ \alpha &= \frac{\pi}{2} - \arctan \frac{x_1}{\rho_0}\end{aligned}$$

Using Eqs. 4 and 5, the field-strength along the x_1 -axis is expressed as follows:

$$E_{x_1} = \frac{M}{2\pi\sigma} \cdot \frac{1}{\rho^3} \left[\cos(\varphi + \alpha) - \sin\varphi \sin\alpha + A \cos(\varphi - \alpha) \right] \quad (\text{Eq. 7})$$

$$\text{where } A = (1 + \gamma\rho) e^{-\gamma\rho}$$

Introducing the above relations between the angles into Eq. 7, gives:

$$F = \frac{1}{4\pi\sigma} \cdot \frac{1}{\rho^3} \left[2A \cos\theta - \cos\theta - 3 \cos\left(\theta - 2 \arctan \frac{x_1}{\rho_0}\right) \right] \quad (\text{Eq. 8})$$

where $F = E_{x1}/M$ is called the transfer-function and expresses the field-strength per unit of dipole moment. It is expressed in the units:

$$\frac{\text{vpm}}{\text{amp-m}} \quad \text{or} \quad \text{ohm/m}^2$$

According to Eq. 8, F is completely determined by the geometrical configuration, as given by θ , ρ_0 and x_1 . The complex factor A in Eq. 7 depends both on the geometry (ρ) and on the frequency, and has to be evaluated when a numerical value of F is required. Eq. 8 shows the interesting fact that F becomes frequency independent for $\theta = \frac{\pi}{2}$.

Factor A can be evaluated as follows:

$$A = (1 + \gamma\rho) e^{-\gamma\rho} ;$$

with

$$\gamma = \frac{1+i}{\delta}$$

and some rearrangements

$$A = e^{-\frac{\rho}{\delta}} \sqrt{2\left(\frac{\rho}{\delta}\right)^2 + 2\frac{\rho}{\delta} + 1} \left[\arctan\left(\frac{\rho/\delta}{1+\rho/\delta}\right) - \frac{\rho}{\delta} \right] \quad (\text{Eq. 9})$$

The skin-depth δ is expressed by Eq. 3, so that the characteristic variable ρ/δ in Eq. 9 can be expressed as:

$$r = \rho/\delta = 0.0019869 \rho \sqrt{f\sigma} \quad (\text{Eq. 10})$$

which transforms Eq. 9 to:

$$A = e^{-r} \sqrt{2r^2 + 2r + 1} \left[\arctan\left(\frac{r}{1+r}\right) - r \right] \quad (\text{Eq. 11})$$

Eq. 11 is introduced into Eq. 8, from which the transfer-function is calculated. A programme was written for the Elliott 503 computer to evaluate the modulus of the transfer-function in the range of $-200 \leq x_1 \leq 200$ m for various combinations of the frequency f , the distances of closest approach ρ_0 , the conductivity σ and the angle θ . The programme is reproduced as Appendix 1, and Fig. 5 shows some examples of calculated transfer-functions.

Even if the case of $\theta = \frac{\pi}{2}$ is covered by Eq. 8, it is worthwhile to consider this case separately. If the field-strength in the y-direction is called E_{y1} , then:

$$E_{y1} = \frac{3M}{2\pi\sigma} \cdot \frac{\rho_0}{\rho^4} \sqrt{1 - \left(\frac{\rho_0}{\delta}\right)^2} \quad (\text{Eq. 12})$$

or, if expressed in terms of ρ_0 and x_1 ,

$$E_{y1} = \frac{3M}{2\pi\sigma} \cdot \rho_0 \cdot x_1 (\rho_0^2 + x_1^2)^{-2.5} \quad (\text{Eq. 13})$$

This expression is completely symmetrical in ρ_0 and x_1 , and shows that E_{y1} is zero when either ρ_0 or x_1 equals zero.

It can furthermore be shown that E_{y1} has a maximum at the point

$$x_1 = \frac{1}{2} \rho_0 \quad (\text{Eq. 14})$$

These interesting characteristics of this component—including its independence of frequency—would facilitate the interpretation of experimentally-determined field-strength. Unfortunately, the practical difficulties of keeping the orientation of transmitter and receiver at exactly 90° are rather large.

From an experimental point of view it is worth considering the relative magnitude of the various horizontal components and their dependence on φ . The expressions from Fig. 2 have been used for an illustration, as shown in Fig. 6. The relative magnitude is expressed in terms of:

$${}^{\prime\prime}F^{\prime\prime} = \frac{{}^{\prime\prime}E^{\prime\prime}}{\frac{M}{2\pi\sigma} \cdot \frac{1}{\rho^3}} \quad (\text{Eq. 15})$$

where ${}^{\prime\prime}E^{\prime\prime}$ represents the components as illustrated in the lower left-hand corner of Fig. 6. The expressions are related in the following way:

$$\left. \begin{aligned} {}^{\prime\prime}F_{\rho}^{\prime\prime} &= \cos \varphi, & {}^{\prime\prime}F_{\varphi}^{\prime\prime} &= 2 \sin \varphi \\ {}^{\prime\prime}F_{\rho}^{\prime\prime} &= {}^{\prime\prime}F_{\varphi}^{\prime\prime} &= 0.9 &\text{ for } \varphi = 26.6^{\circ} \\ {}^{\prime\prime}F_x^{\prime\prime} &= 1 - 3 \sin^2 \varphi, & {}^{\prime\prime}F_y^{\prime\prime} &= \frac{3}{2} \sin 2\varphi \\ {}^{\prime\prime}F_x^{\prime\prime} &= 0 &&\text{ for } \varphi = 35.3^{\circ} \\ {}^{\prime\prime}F_h^{\prime\prime} &= \sqrt{{}^{\prime\prime}F_{\rho}^{\prime\prime}{}^2 + {}^{\prime\prime}F_{\varphi}^{\prime\prime}{}^2} = \sqrt{{}^{\prime\prime}F_x^{\prime\prime}{}^2 + {}^{\prime\prime}F_y^{\prime\prime}{}^2} = \sqrt{1 + 3 \sin^2 \varphi} \end{aligned} \right\} (\text{Eq. 16})$$

In connection with Eq. 16 and Fig. 6, it is worth mentioning that, with two perpendicular electrode systems, it is not possible to determine the direction from the point of observation to the transmitting dipole by means of a single measurement, unless the relative orientation between the transmitter and the electrode systems is already known. This property of the near fields creates the practical problem of keeping track of position and orientation during experiments.

1.2 Corrections for Discontinuities

So far, all the expressions given for the field-strength have been computed for the condition of a conducting half-space. Since this condition cannot always be fulfilled during experiments, two special cases of discontinuities have been considered and the appropriate corrections found.

The first case is the influence of the sea-bed on the propagation, and thus on the field-strength as measured at the point of observation. The model considered consists of a conducting sea of conductivity $\sigma_1 = \sigma$ and of depth d . Fig. 7 illustrates the situation. The formal approach is to derive the fields from a Hertz-vector having x and z component and satisfying the proper boundary conditions at $z = 0$ and $z = d$.

The rather complicated expressions can be simplified if one assumes that the conductivity of the sea-bed is sufficiently low, and that the ranges are small compared with the wavelength in air and in the sea-bed. With reference to Eqs. 1 and 2 this means that $\gamma_0 = \gamma_2 \approx 0$. A further simplification is made by assuming that the range is large compared with the water wavelength, and that the transmitter and the receiver are at the surface.

Under these circumstances it is found that, to the first order approximation, the sea-bed at depth d contributes a correction factor

$$1 + 2e^{-2\gamma d} \quad (\text{Eq. 17})$$

to the field for an infinitely deep sea. The transmission path for this situation is also shown in Fig. 7. The direct path from the transmitter to the receiver is the same as before. The indirect path, where the signal travels through the sea-bed, contains a total water-path of length $2d$. Apart from the phase-shift, this part of

the signal will receive an attenuation of $e^{-\frac{2d}{\delta}}$, where δ is the skin-depth.

The factor 2 in front of the exponential can be explained by referring to Fig. 7. If the transmitting dipole is raised towards the surface, its first image, as shown by the broken line, is lowered towards the surface and finally coincides with the dipole. Seen from the conducting medium this means that the strength of the dipole is doubled. (This point of view agrees with optics: when a light ray is reflected by a denser medium there is a phase-shift of 180° . However, if the ray comes from the denser medium and is reflected by the interface with a less dense medium no phase-shift occurs.)

The correction factor of Eq. 17 is written in the following way:

$$A' = 1 + 2e^{-2\gamma d} = 1 + 2e^{-\frac{2d}{\delta}(1+i)} = 1 + 2e^{-a(1+i)} \quad (\text{Eq. 18})$$

A plot of the function A' is shown in Fig. 8. The modulus is given by the length of the vector from the origin to a point on the curve, which is labelled with various values of $a = 2d/\delta$. As seen from the curve, there is a considerable enhancement of the signal when the water-depth is small in comparison with the skin-depth. The factor has a minimum for $a \sim 2.5$ ($d \sim 1.25 \delta$).

The second case of discontinuity, which will be discussed briefly, is the influence of the platform used for the measurement of EM fields. During the earlier parts of the programme, the island of Tino in the Gulf of La Spezia was the site of two measuring stations. A more detailed description of the equipment used for the measurement of EM background noise is given in the second report of this series (T.R. 37). The stations were also used during propagation experiments with the same equipment, when one of the horizontal magnetic components in air was measured. The influence of the island on the fields to be measured has been

calculated in terms of a very simple model. The following is a brief outline of the procedure, together with some final results.

The treatment of the problem makes use of the model shown in Fig. 9, and follows the procedure of Kaden (Ref. 5). The model consists of an infinitely thin plate having infinite conductivity and containing a hole of radius r_0 . In the half-space above the plate there is a vertical electric field E_z , which, at great distance from the hole, has the value E_0 . The field close to the hole will be disturbed by the presence of the hole, with the result that the field penetrates into the half-space below the plate. The problem consists of computing the field E_z in the neighbourhood of the hole.

In relation to the actual situation at the island of Tino this crude model is acceptable. The sea around Tino is 10 - 30 m deep, which is small compared with the horizontal dimensions of Tino — which can be approximated by a circle of radius $r_0 = 200$ m. In comparison, the sea can thus be considered as an infinitely thin plate. As to conductivity, it is assumed that Tino has nearly the same properties as air, so that the conductivity of the sea is very much greater than that of the island. Apart from the top layer, the island consists of marble, the conductivity of which is about 10^{-8} times that of seawater.

Kaden (Ref. 5, p. 222) gives the solution to the problem as a closed expression in elliptical co-ordinates:

$$\underline{E} = \text{grad } X$$

where

$$X = \frac{E_0 r_0}{\pi} \cdot \eta \left[\xi \left(\arctan \xi + \frac{\pi}{2} \right) + 1 \right] \quad (\text{Eq. 19})$$

in which the elliptical co-ordinates (ξ, η) are related to the cylindrical co-ordinates (ρ, z) in the following way:

$$\left. \begin{aligned} \rho^2 &= r_0^2 (1 + \xi^2)(1 - \eta^2) \\ z &= r_0 \cdot \xi \cdot \eta \\ 0 \leq \eta \leq 1, \quad -\infty < \xi < \infty \end{aligned} \right\} \quad (\text{Eq. 20})$$

The φ -co-ordinate is neglected because of the symmetry of rotation.

The z-component of the gradient is then expressed in terms of the elliptic components, yielding the following final expression:

$$\frac{E_z}{E_0} = \frac{1}{\pi} \left[\arctan \xi + \frac{\pi}{2} + \frac{\xi}{\xi^2 + \eta^2} \right] \quad (\text{Eq. 21})$$

In a similar way, the horizontal magnetic field parallel to the plate is given by Kaden (Ref. 5, p. 250) as

$$\underline{H} = \text{grad } X$$

$$X = \frac{1}{2} H_0 \rho \left[1 + \frac{2}{\pi} \left(\arctan \xi + \frac{\xi}{1 + \xi^2} \right) \right] \cos \varphi \quad (\text{Eq. 22})$$

where φ is the angle between the radius vector and the direction of the magnetic field. Expressing the x-component in terms of elliptical components yields the final expression

$$\frac{H_x}{H_0} = \frac{1}{\pi} \left[\arctan \xi + \frac{\pi}{2} + \frac{\xi}{1 + \xi^2} \right] \quad (\text{Eq. 23})$$

which is very similar to Eq. 21.

Numerical values for certain points of observation have been computed on the basis of an approximation of the island's proportions. Fig. 10 shows the west-east cross-section of Tino in full line and indicates the positions of the two stations, A and B. The approximation used is shown by the dimensions of the dotted lines.

Fig. 11 shows the corresponding values for H_x/H_o and E_z/E_o at various points on the model of the island, the co-ordinates (ξ, η) of which are given in brackets. The most interesting part is H_x/H_o , which has a value of about 0.76 at station A and of about 0.5 at station B. This has been observed experimentally by simultaneous measurements of the magnetic component of the background noise at A and B. The value of E_z/E_o at station A is close to 1. This approach does not permit the calculation of the ratio at station B and another model would have to be considered for this case.

Similar effects occur where the measuring place is surrounded by mountains — in fjords and lochs for example.

1.3 Transient Excitation

So far, the fields have been calculated on the basis of sinusoidal excitation of the dipole. Many of the phenomena to be studied — the background noise, for example — are, however, of impulsive character and it was thought necessary to study the medium under the condition of transient excitation of the dipole.

The treatment was based on Laplace transform theory, and assumed a dipole excited by a step-function current in the conducting medium. A paper by

Mijnarends (Ref. 6) gives details of the treatment and the limits of validity of the expressions. Besides the electric and magnetic components in the conducting medium, the vertical electric field in air E_{oz} at various points on the surface was examined. Since the expressions are rather involved, numerical results are given only for E_{oz} and H_{1x} .

The response of E_{oz} is a pulse with a rise-time proportional to the square of the depth of the dipole but independent of the horizontal distance, and with a long trailing edge. The magnetic component H_{1x} rises slowly to a stationary value. Its rise-time increases with increasing horizontal distance. It is also shown that there is a marked difference in attenuation with depth — and sometimes also with horizontal distance — between transient and sinusoidal signals. Some of the results obtained could be checked against the results obtained by Wait (Ref. 7) who used exponential and bell-shaped source functions.

During the course of this study it was also found that the frequency response of the detecting equipment has to be taken into account when determining the range dependence. This is of importance for propagation experiments. The following general hypothesis, the validity of which has not been proven experimentally due to lack of time, has been suggested. Consider a transient disturbance of the electromagnetic field propagating over a highly conducting half-space. If it depends on no other distance than the horizontal distance, ρ , between the transmitter and detector, and if its amplitude is proportional to $\rho^{-\alpha}$, then, if it is detected with a detector having a frequency response proportional to ω^β , the output of the detector will depend on horizontal range as $\rho^{-(\alpha+2\beta)}$.

It was shown in the previous section that the field is influenced by the presence of the sea-bed and the non-conducting island. It was also shown that, in the sinusoidal case, the influence of the sea-bed could be expressed in terms of a

correction factor depending on the ratio of the water-depth to the skin-depth. A similar influence will be present in the case of transient excitation. If the transient is expressed in the frequency domain it is seen that the presence of the sea-bed will enhance the amplitude of the low-frequency part of the signal, where the water-depth is small compared with the skin-depth. The high frequency parts will be attenuated in the water-path, and there will be no change from the half-space condition. The waveshape at the point of observation will thus look different from the waveshape computed on the basis of Ref. 6.

2. THE EM FIELD FROM FINITE ANTENNAS

The radiation from a finite antenna in a conducting medium has received attention from several authors. In general, the antenna is described as an insulated wire connected to the conducting medium through electrodes that have small dimensions but that effectively short-circuit the wire. Under these circumstances the dipole moment of the antenna is $I_0 \cdot \ell$, where the current, I_0 , is constant along the wire and ℓ is the length.

The fields from such an antenna can thus be computed in the same way as those from the infinitesimal dipole, provided that the horizontal distance ρ' , as measured from the nearest part of the antenna, fulfills the conditions of the propagation law used. The contribution of the electrode to the dipole moment is generally neglected by assuming that the electrodes are spheres having a radius that is small in comparison with the skin-depth.

However, spherical electrodes are not used for practical transmitting antennas at sea. Instead one uses the so-called "short-circuited coaxial antenna", in which the extension of the centre-conductor is in contact with the sea. Such an antenna was described, for example, by Moore (Ref. 8), who, however, also neglected the radiation from the bare wire. This is not generally permissible, and an attempt was made to determine this radiation and to find the corresponding dipole moment.

This problem was approached according to Fig. 12, which shows a coaxial antenna oriented along the z' -axis, with its insulated part extending from the origin to ℓ and the bare parts from ℓ to $\ell + L$. The point of observation is P, and the distance between P and a point z' is approximated by:

$$R' \approx R - z' \cos \theta \quad (\text{Eq. 24})$$

which is valid for R and $R' \gg \ell + L$. (The drawing in Fig. 12 does not fulfill this condition).

For an elementary dipole one has the Herz potential

$$\Pi_z = \frac{I_0 \ell}{4\pi R \sigma} e^{-\gamma R} \quad (\text{Eq. 25})$$

For the insulated part of the short-circuited coaxial antenna this gives:

$$\Pi_{z, \text{ins}}^{\text{sc}} = \frac{I_0 e^{-\gamma R}}{4\pi \sigma R \gamma \cos \theta} (e^{\gamma \ell \cos \theta} - 1) \quad (\text{Eq. 26})$$

For the uninsulated part, the attenuation of the current is the same as that of a plane wave in sea-water. Since L is rather small, however, there will be a reflection from the end at $z' = \ell + L$; this depends on the load impedance, which is rather uncertain and is difficult to calculate.

For estimating the magnitude, two extreme cases are considered: (1) where the bare wire is treated as open-circuited transmission line, and (2) where the bare wire is equivalent to a short-circuited transmission line. In both cases the current $I(z')$ in the bare wire can be found from transmission line theory:

(1) Open circuit

$$I(z') = I_0 \frac{\sinh[\gamma(L + \ell - z')]}{\sinh \gamma L} \quad (\text{Eq. 27})$$

(2) Short circuit

$$I(z') = I_0 \frac{\cosh[\gamma(L+\ell-z')]}{\cosh \gamma L} \quad (\text{Eq. 28})$$

The Herz potential of the bare wire is found using each of these currents. When added to the Herz potential of the insulated part the following results are obtained:

$$(1) \quad \prod_{z, \text{total}}^{\text{sc}(\text{oc})} = \frac{I_0 \ell e^{-\gamma R}}{4\pi\sigma R} \left(1 + \frac{\cosh \gamma L - 1}{\gamma \ell \sinh \gamma L} \right) \quad (\text{Eq. 29})$$

$$(2) \quad \prod_{z, \text{total}}^{\text{sc}(\text{sc})} = \frac{I_0 \ell e^{-\gamma R}}{4\pi\sigma R} \left(1 + \frac{\tanh \gamma L}{\gamma \ell} \right) \quad (\text{Eq. 30})$$

If $\gamma L \ll 1$, the term in brackets in Eq. 29 is approximately equal to $1 + (L/2\ell)$. Similarly for Eq. 30 the term in brackets is approximately equal to $1 + L/\ell$. Comparing these results with Eq. 25, it follows that, for the short-circuited coaxial antenna, the equivalent dipole moment is equal to:

$$(I \ell)^{\text{sc}} = I_0 (\ell + \alpha L) \quad (\text{Eq. 31})$$

where the factor α depends on whether the bare end must be considered as a short-circuited transmission line ($\alpha = 1$), an open-circuited transmission line ($\alpha = 0.5$), or something in between ($0.5 < \alpha < 1$). In designing an antenna one would generally select the case of $\alpha = 1$ and determine L as a function of ℓ in such a way that the bare part constitutes a short-circuit for the coaxial antenna. If, for example $L > \frac{1}{8} \lambda_{\text{water}}$ and $\ell = 100$ m, then it was found that $L = 25$ m would satisfy the conditions for frequencies of 60 cps and above.

3. ESTIMATE OF THE ACCURACY OF FIELD-STRENGTH CALCULATIONS AND MEASUREMENTS

The expressions for the field from a horizontal dipole in the conducting medium have been treated in section 2.1. As mentioned, these expressions are valid for a conducting half-space, and corrections for discontinuities were derived in section 2.2. In all cases the expressions are the result of approximations introduced to facilitate the mathematics and to obtain solutions in a closed form. From the point of view of the experimenter, these various approximations obscure the picture and make it difficult to determine whether deviations from a theoretical result are due to measuring errors or to a built-in inaccuracy in the expressions.

An estimate of the accuracy of these various expressions has therefore been made. Such an investigation is rather involved, and the estimate was performed only for the horizontal electric component in the conducting medium. The results are presented in Figs. 13 and 14.

The ρ - z half-plane, where ρ and z are expressed in terms of skin-depth, is basically divided by two curves A and B. At points on these curves, the modulus of the field due to direct transmission is equal to the modulus of the field due to the transmission path along the surface and perpendicularly downwards. The actual field-strength measured on the curves depends on the phase relationship between the two transmission paths. This phase relationship can create maxima and minima, and the dotted lines indicate where one or the other of the fields is predominant and where the expressions shown can be used subject to the approximation introduced. The error-limits have been chosen, rather arbitrarily, at $\pm 4\%$ and $\pm 40\%$, and thereby suggest which regions should be avoided during experiments if one wants to check measured results against theoretical expressions.

4. EXPERIMENTS CONCERNING EM-FIELDS AND PROPAGATION

Propagation experiments and the measurements of field-strength have been mentioned several times in this report. There were several reasons for performing these experiments. Firstly, the difficult relationships between the various parts of the EM field makes this an interesting subject for experiments that provide a good introduction to the whole topic.

The second reason, which may be of even greater importance, is related to the measurement of EM background noise. If the background noise is to be measured at absolute levels, some kind of calibration of the measuring equipment is needed. In general, it is quite easy to determine the amplification of the equipment by introducing a known signal across the detector and measuring the output, but this system, which is widely used by experimenters, does not take the detector itself into account. One exception is the magnetic detector, which can be surrounded by a coil or a set of coils (for example, Helmholtz-coil systems) with which a known field is created. However, this is not suitable for use at sea, nor is it applicable to extended electrode systems. The propagation experiment is, therefore, a means of calibrating the measuring system on the basis of a known dipole moment and the known relative positions of transmitting dipole and receiver.

It should, however, be kept in mind that this way of calibrating is, in fact, only good for nearby signals, and the question arises as to what conclusions can be drawn with respect to the source of background noise arising from far-off signals on the basis of the calibration with nearby signals. In clean geometry, the answer is that it should be fairly safe to calibrate the detector in this way when far from coastlines and over deep water. The polarization of the background-noise field and the orientation of the receiver must, however, be kept in mind.

The accuracy of such a calibration depends on a number of factors, one being the error of approximation in the expressions for the field-strength, as already mentioned in Section 4. Other factors deal with the relative positions of transmitter and receiver, since the angle dependence of the components requires a knowledge of the relative angle between transmitter and receiver, as shown in Section 2.1. A further source of error is the horizontal distance ρ . As seen from various expressions, ρ generally appears in terms of ρ^n , where n is usually 3. This means that a relative error of 10% in the measurement of ρ introduces a relative error of 30% in the field-strength measured. From a practical point of view, this source of error is probably the most serious one, and has to be taken into account when comparing experimental results.

An example of a typical propagation experiment is shown in Figs. 15 and 16. The experiment was performed with a dipole excited by short pulses, as shown in Fig. 15. The pulses are generated in a transistorized pulse-generator triggered by a low-frequency oscillator. The width of the pulses at their base is about 40 ms and does not vary greatly when the pulse repetition frequency is changed. The relative level of harmonics, therefore, varies with frequency. In the present case the repetition frequency was 10 cps. The upper cut-off frequency of the equipment was set at about 30 cps, so that only the 10 and 20 cps components are of importance.

The experiments were performed in the following way. The receiver electrode system was suspended from a raft to a depth of about 10 m, which corresponds to $1/8$ and $1/5$ of a skin-depth of 10 and 20 cps respectively. No corrections were made for the attenuation due to the depth. The transmitting dipole was towed behind a small boat on a constant course and at a constant speed. An attempt was made to keep the course parallel to the receiving electrode system, the distance of closest approach being 40 m. The received signal was recorded on

tape, and the rms-values of the frequency components of the field-strength were determined at different points along a track by power spectrum analysis. The rms-values of the dipole moment at the various frequencies were found from a spectrum analysis of the transmitting current. The transfer-function $|E/M|$ was then computed in rms values of $\frac{\text{vpm}}{\text{amp-m}}$.

The experimental points are shown in Fig. 16, together with the curves representing the transfer-function under the given geometrical conditions. There is reasonable agreement between experiment and calculation. It should, however, be kept in mind that in this case the calculations have been performed for a conducting half-space. In fact, the water-depth at the measuring place was only 100-150 m. This fact could eventually explain why the 20 cps points fit the curve somewhat better than the 10 cps points.

The propagation experiments described made use of the latest equipment developed by the EM Group. This equipment will be described in detail in the second report of this same series (T.R. 37).

REFERENCES

- (1) L. Brock-Nannestad, "Bibliography of EM Phenomena with Special Reference to ELF (1-300 cps)", NATO SACLANTCEN, T.R. 25, October 1964.
- (2) A. Banos, Jr. and J.P. Wesley, "The Horizontal Electric Dipole in a Conducting Half-Space", SIO Ref. 53-33, September 1953.
- (3) A.N. Sommerfeld, Ann. Physik, Vol. 81, 1926, p. 1135.
- (4) J.R. Wait, "The EM Fields of a Horizontal Dipole in the Presence of a Conducting Half-Space", Canadian J. of Physics, Vol. 39, 1961, p. 1017.
- (5) H. Kaden, "Wirbelströme und Schirmung in der Nachrichtentechnik", Zweite Auflage, Springer Verlag 1959, pp. 222 and 250.
- (6) P.E. Mijnaerends, "Propagation of Electromagnetic Step Functions over a Conducting Medium", J. Appl. Phys. (USA), Vol. 33, No. 8, August 1962, pp. 2556-64.
- (7) J.R. Wait, "Propagation of Electromagnetic Pulses in a Homogeneous Conducting Earth", Appl. Sci. Res. (Netherlands), Section B, Vol. 8, 1960, pp. 213-253.
- (8) R.K. Moore, "The Theory of Radio Communication Between Submerged Submarines", Ph. D. Thesis, Cornell University, 1951.

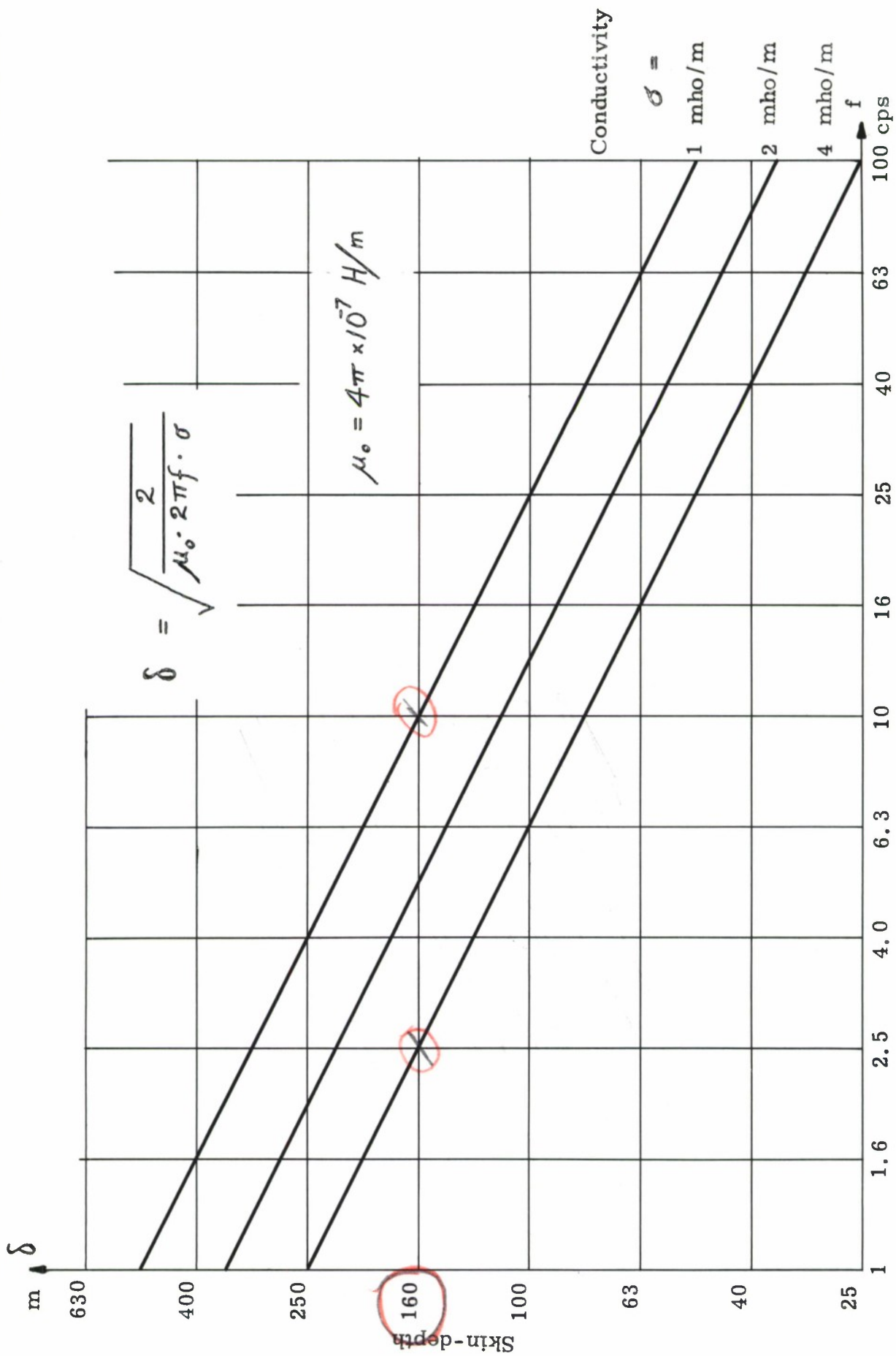


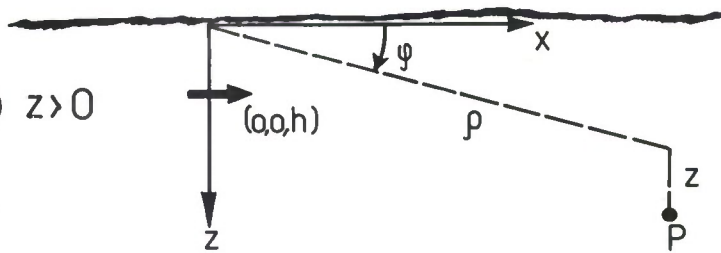
Fig. 1

Skin-depth, δ , as a function of the relevant frequencies for various conductivity values typical of sea-water

NEAR FIELDS OF HORIZONTAL DIPOLES

① $z < 0$

② $z > 0$



$$\gamma = (i\mu\omega\sigma)^{\frac{1}{2}}$$

$$= \frac{\sqrt{2}}{\delta} e^{\frac{\pi}{4}i}$$

δ = skin depth

ELECTRIC DIPOLE

$$E_{0\rho} = \frac{Idl}{2\pi\sigma} \frac{1}{\rho^3} (1+\gamma z) \cos\varphi e^{-\gamma h}$$

$$H_{0\rho} = -\frac{Idl}{2\pi\gamma} \frac{1}{\rho^3} 2\sin\varphi e^{-\gamma h}$$

$$E_{0\varphi} = \frac{Idl}{2\pi\sigma} \frac{1}{\rho^3} (2-\gamma z) \sin\varphi e^{-\gamma h}$$

$$H_{0\varphi} = \frac{Idl}{2\pi\gamma} \frac{1}{\rho^3} \cos\varphi e^{-\gamma h}$$

$$E_{0z} = -\frac{Idl}{2\pi\sigma} \frac{1}{\rho^3} (\gamma\rho) \cos\varphi e^{-\gamma h}$$

$$H_{0z} = -\frac{Idl}{2\pi\gamma} \frac{1}{\rho^3} \left(\frac{3}{\gamma\rho}\right) (1-\gamma z) \sin\varphi e^{-\gamma h}$$

$$E_{1\rho} = \frac{Idl}{2\pi\sigma} \frac{1}{\rho^3} \cos\varphi e^{-\gamma(z+h)}$$

$$H_{1\rho} = -\frac{Idl}{2\pi\gamma} \frac{1}{\rho^3} 2\sin\varphi e^{-\gamma(z+h)}$$

$$E_{1\varphi} = \frac{Idl}{2\pi\sigma} \frac{1}{\rho^3} 2\sin\varphi e^{-\gamma(z+h)}$$

$$H_{1\varphi} = \frac{Idl}{2\pi\gamma} \frac{1}{\rho^3} \cos\varphi e^{-\gamma(z+h)}$$

$$E_{1z} \approx 0$$

$$H_{1z} = \frac{Idl}{2\pi\gamma} \frac{1}{\rho^3} \left(\frac{3}{\gamma\rho}\right) \sin\varphi e^{-\gamma(z+h)}$$

MAGNETIC DIPOLE

$$E_{0\rho} = \frac{IdA}{2\pi\sigma} \frac{\gamma}{\rho^3} (1+\gamma z) \sin\varphi e^{-\gamma h}$$

$$H_{0\rho} = \frac{IdA}{2\pi} \frac{1}{\rho^3} 2\cos\varphi e^{-\gamma h}$$

$$E_{0\varphi} = -\frac{IdA}{2\pi\sigma} \frac{\gamma}{\rho^3} (2-\gamma z) \cos\varphi e^{-\gamma h}$$

$$H_{0\varphi} = \frac{IdA}{2\pi} \frac{1}{\rho^3} \sin\varphi e^{-\gamma h}$$

$$E_{0z} = -\frac{IdA}{2\pi\sigma} \frac{\gamma}{\rho^3} (\gamma\rho) \sin\varphi e^{-\gamma h}$$

$$H_{0z} = -\frac{IdA}{2\pi} \frac{1}{\rho^3} \left(\frac{3}{\gamma\rho}\right) (1-\gamma z) \cos\varphi e^{-\gamma h}$$

$$E_{1\rho} = \frac{IdA}{2\pi\sigma} \frac{\gamma}{\rho^3} \sin\varphi e^{-\gamma(z+h)}$$

$$H_{1\rho} = \frac{IdA}{2\pi} \frac{1}{\rho^3} 2\cos\varphi e^{-\gamma(z+h)}$$

$$E_{1\varphi} = -\frac{IdA}{2\pi\sigma} \frac{\gamma}{\rho^3} 2\cos\varphi e^{-\gamma(z+h)}$$

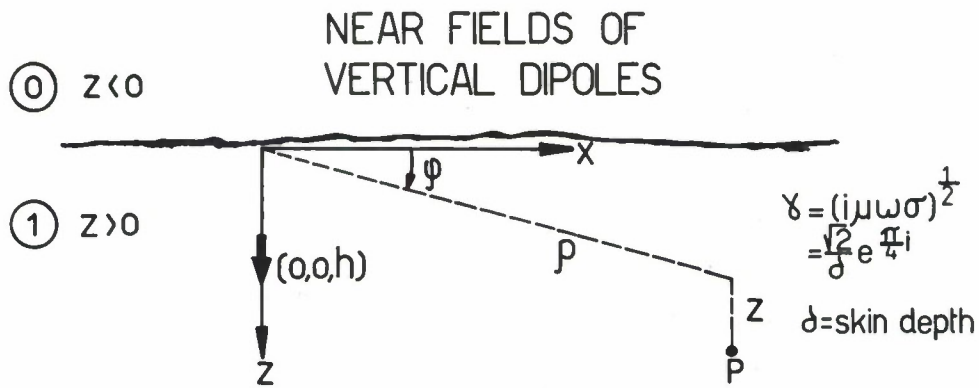
$$H_{1\varphi} = -\frac{IdA}{2\pi} \frac{1}{\rho^3} \sin\varphi e^{-\gamma(z+h)}$$

$$E_{1z} \approx 0$$

$$H_{1z} = -\frac{IdA}{2\pi} \frac{1}{\rho^3} \left(\frac{3}{\gamma\rho}\right) \cos\varphi e^{-\gamma(z+h)}$$

Range of validity: $\lambda_{\text{water}} \ll \rho \ll \lambda_{\text{air}}$
MKS units

Fig. 2



ELECTRIC DIPOLE

$$E_{0\rho} = \frac{3Idl}{2\pi\sigma} \frac{z}{\rho^4} e^{-\gamma h}$$

$$H_{0\rho} \equiv 0$$

$$E_{0\phi} \equiv 0$$

$$H_{0\phi} \approx 0$$

$$E_{0z} = -\frac{Idl}{2\pi\sigma} \frac{1}{\rho^3} e^{-\gamma h}$$

$$H_{0z} \equiv 0$$

$$E_{1\rho} \approx 0$$

$$H_{1\rho} \equiv 0$$

$$E_{1\phi} \equiv 0$$

$$H_{1\phi} \approx 0$$

$$E_{1z} \approx 0$$

$$H_{1z} \equiv 0$$

MAGNETIC DIPOLE

$$E_{0\rho} \equiv 0$$

$$H_{0\rho} = \frac{3IdA}{2\pi\gamma} \frac{1}{\rho^4} e^{-\gamma h}$$

$$E_{0\phi} = -\frac{3IdA}{2\pi\sigma} \frac{1}{\rho^4} (1-\gamma z) e^{-\gamma h}$$

$$H_{0\phi} \equiv 0$$

$$E_{0z} \equiv 0$$

$$H_{0z} = -\frac{IdA}{2\pi\gamma} \frac{1}{\rho^4} \left(\frac{9}{\gamma\rho} \right) (1-\gamma z) e^{-\gamma h}$$

$$E_{1\rho} \equiv 0$$

$$H_{1\rho} = \frac{3IdA}{2\pi\gamma} \frac{1}{\rho^4} e^{-\gamma(z+h)}$$

$$E_{1\phi} = -\frac{3IdA}{2\pi\sigma} \frac{1}{\rho^4} e^{-\gamma(z+h)}$$

$$H_{1\phi} \equiv 0$$

$$E_{1z} \equiv 0$$

$$H_{1z} = -\frac{IdA}{2\pi\gamma} \frac{1}{\rho^4} \left(\frac{9}{\gamma\rho} \right) e^{-\gamma(z+h)}$$

Range of validity: $\lambda_{\text{water}} \ll \rho \ll \lambda_{\text{air}}$
MKS units

Fig. 3

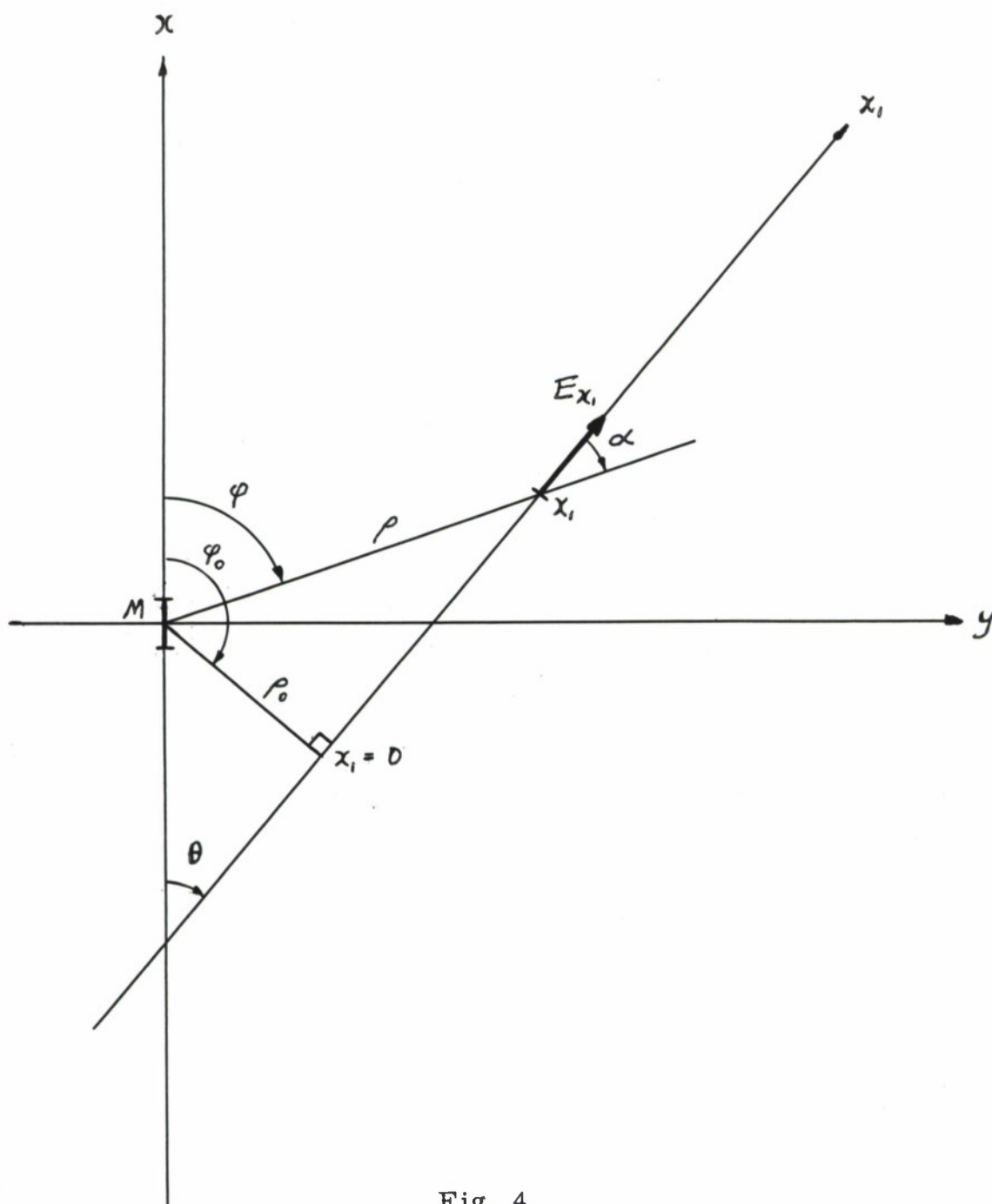


Fig. 4

Geometry of the measurements of horizontal field strength; seen
from above the surface

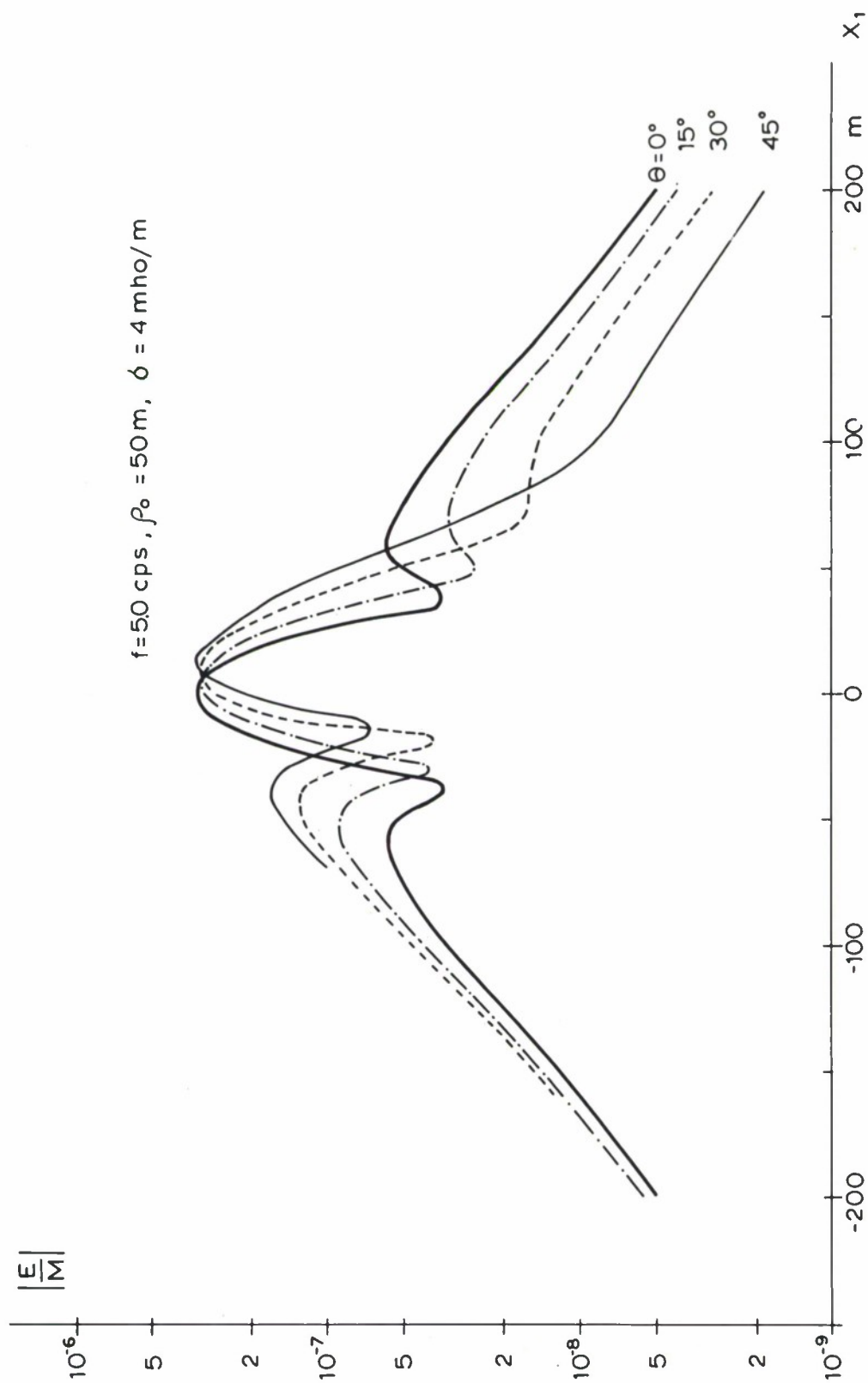


Fig. 5 Modulus of the transfer function E_{x_1}/M as a function of x_1 and with θ as a parameter.

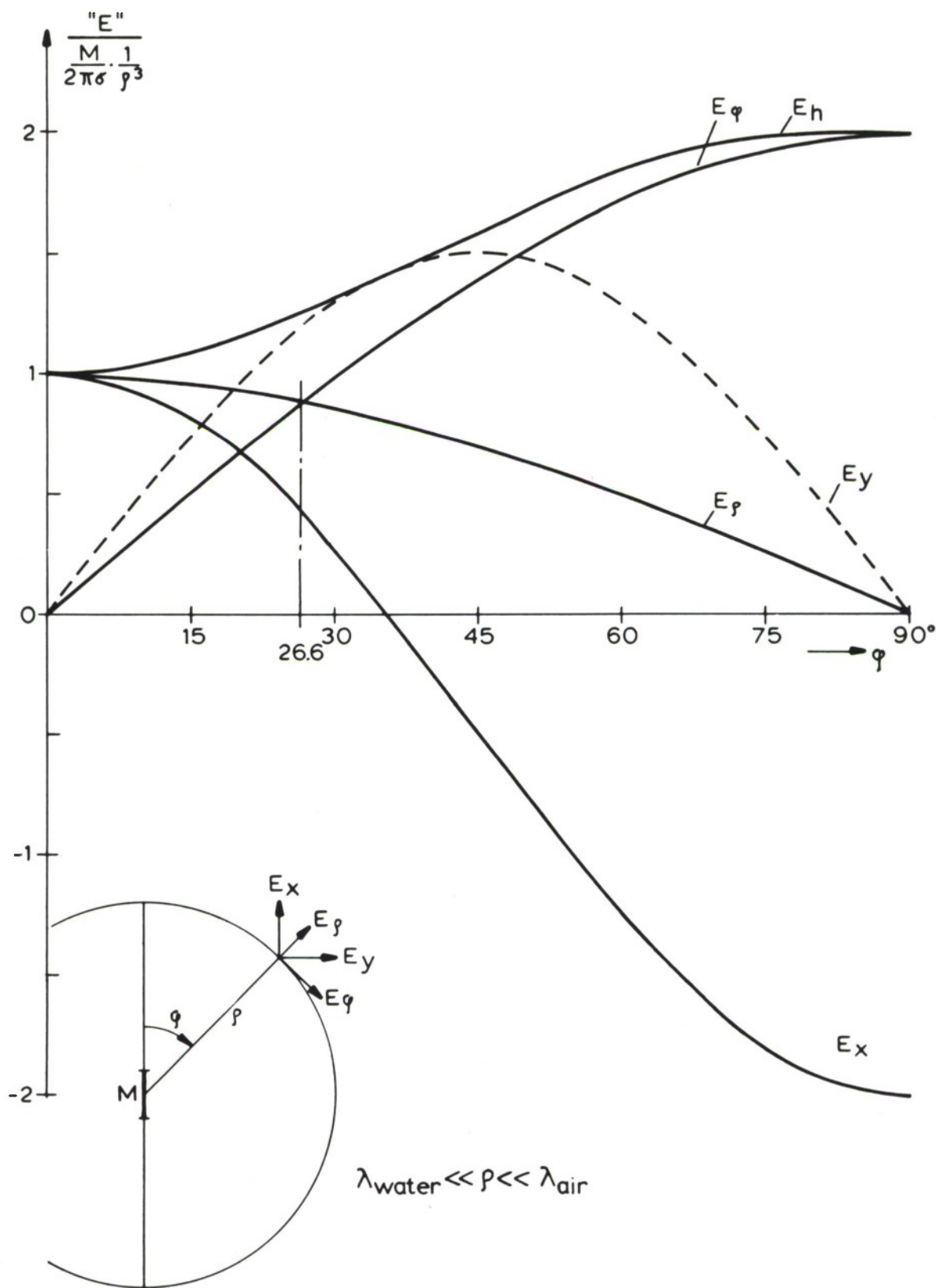


Fig. 6 The angle dependence of the horizontal E components at the surface and where $|\gamma\rho| \gg 1$.

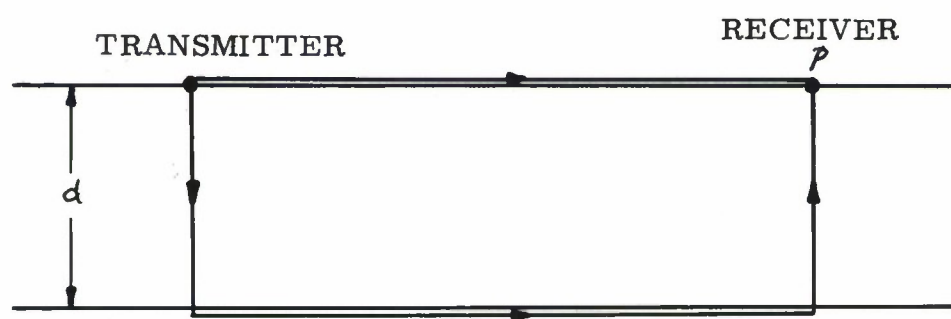
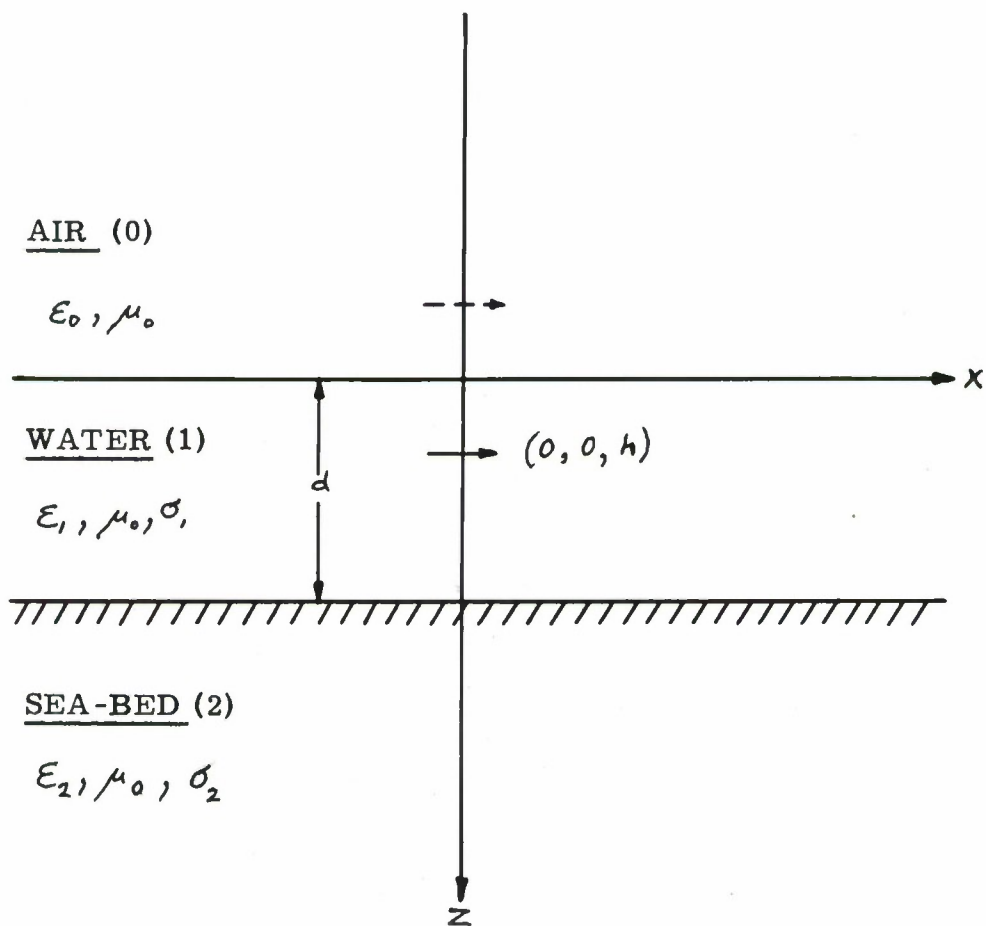


Fig. 7

The influence of the sea-bed on propagation

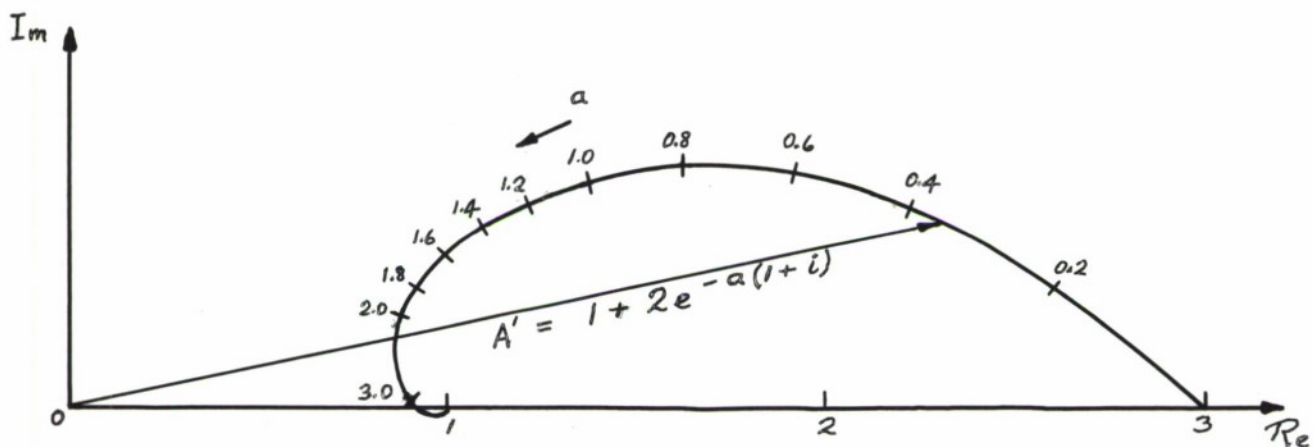


Fig. 8

Correction factor for use with limited water-depths

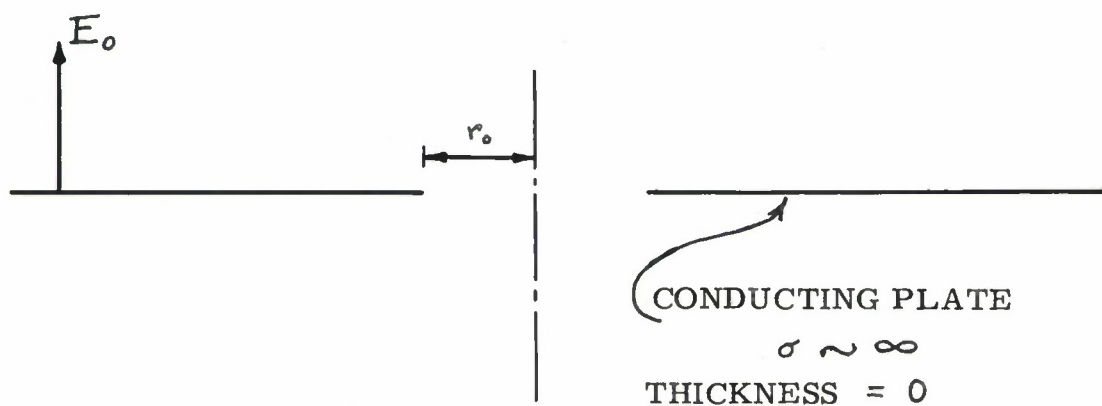


Fig. 9

An infinitely thin conducting plate with a round hole — used as a model of an insulating island in an ocean

west

east

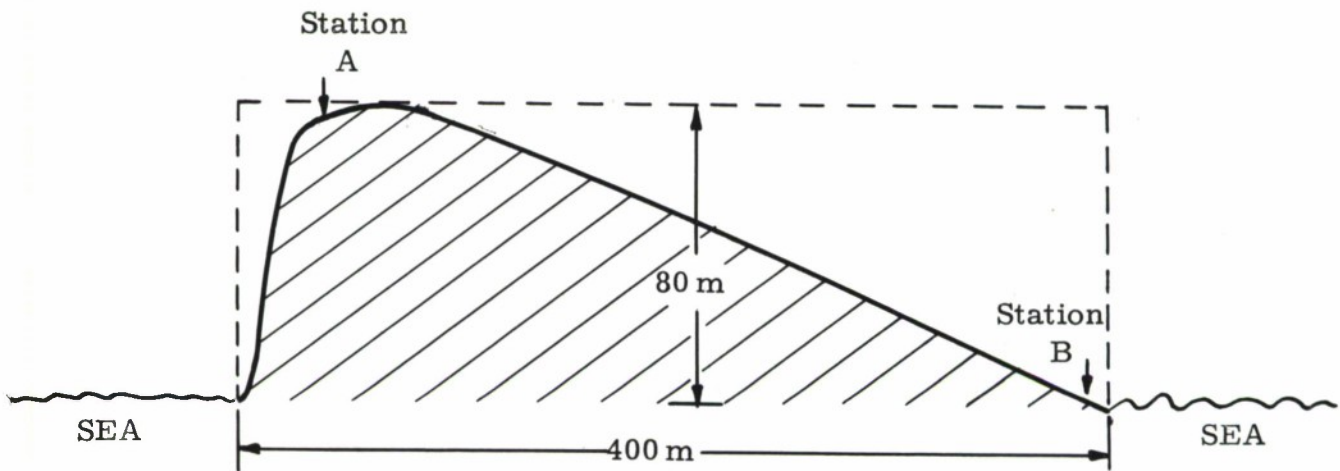


Fig. 10

West-east cross section of the island of Tino (Gulf of La Spezia), showing positions of the two stations and the approximation used

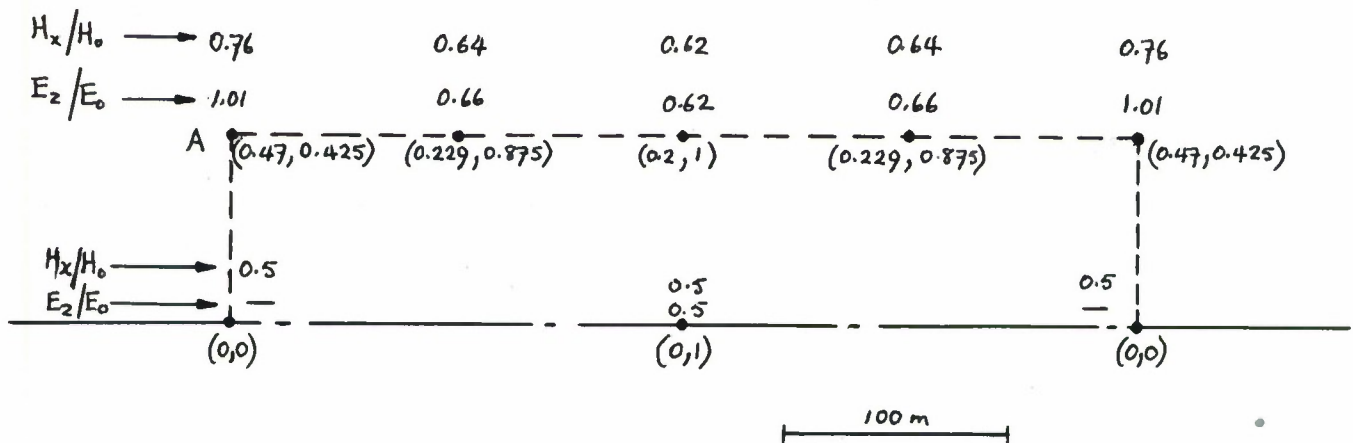


Fig. 11

Values of H_x/H_0 and E_z/E_0 at various points on the model of the island of Tino

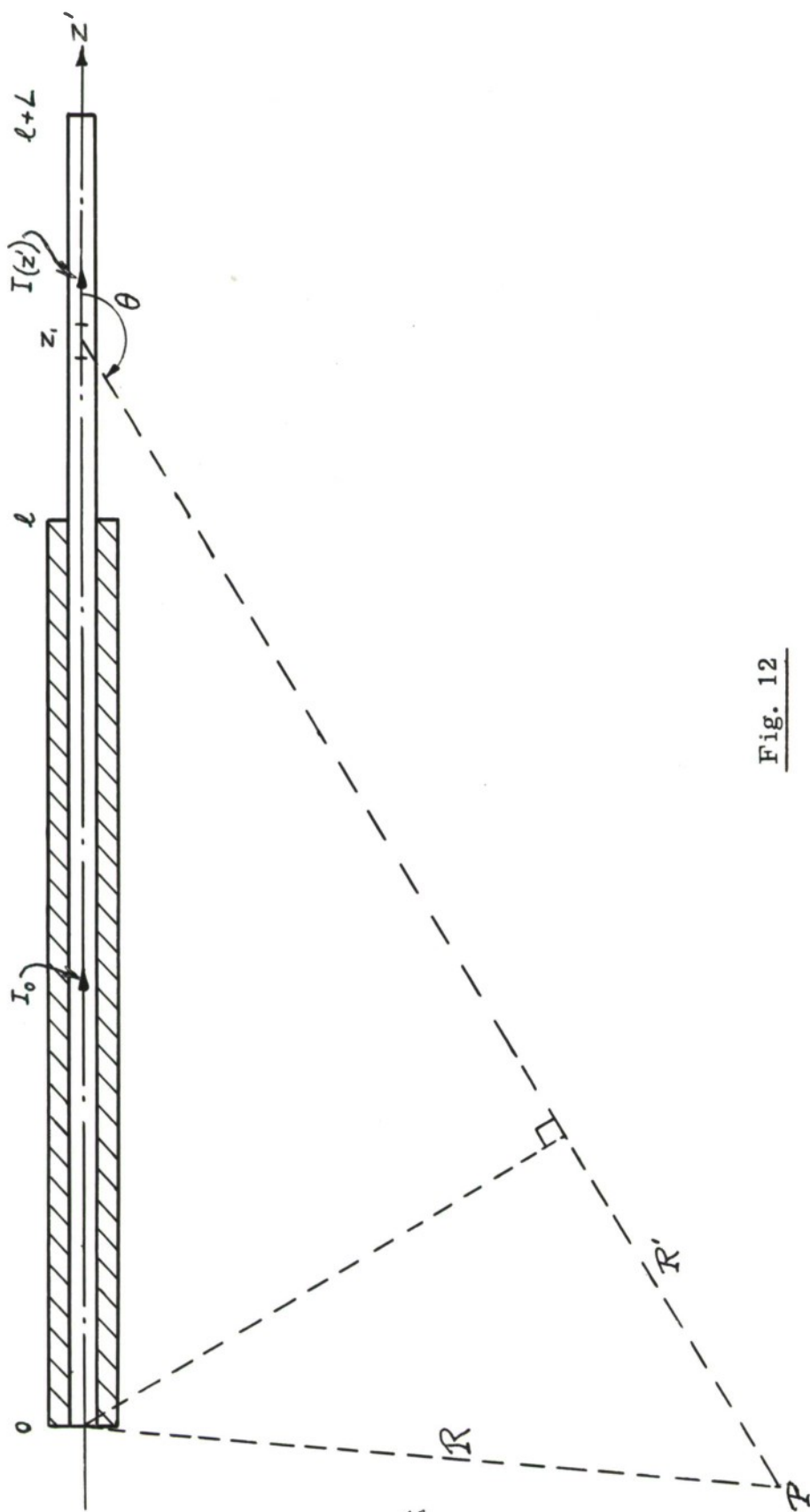
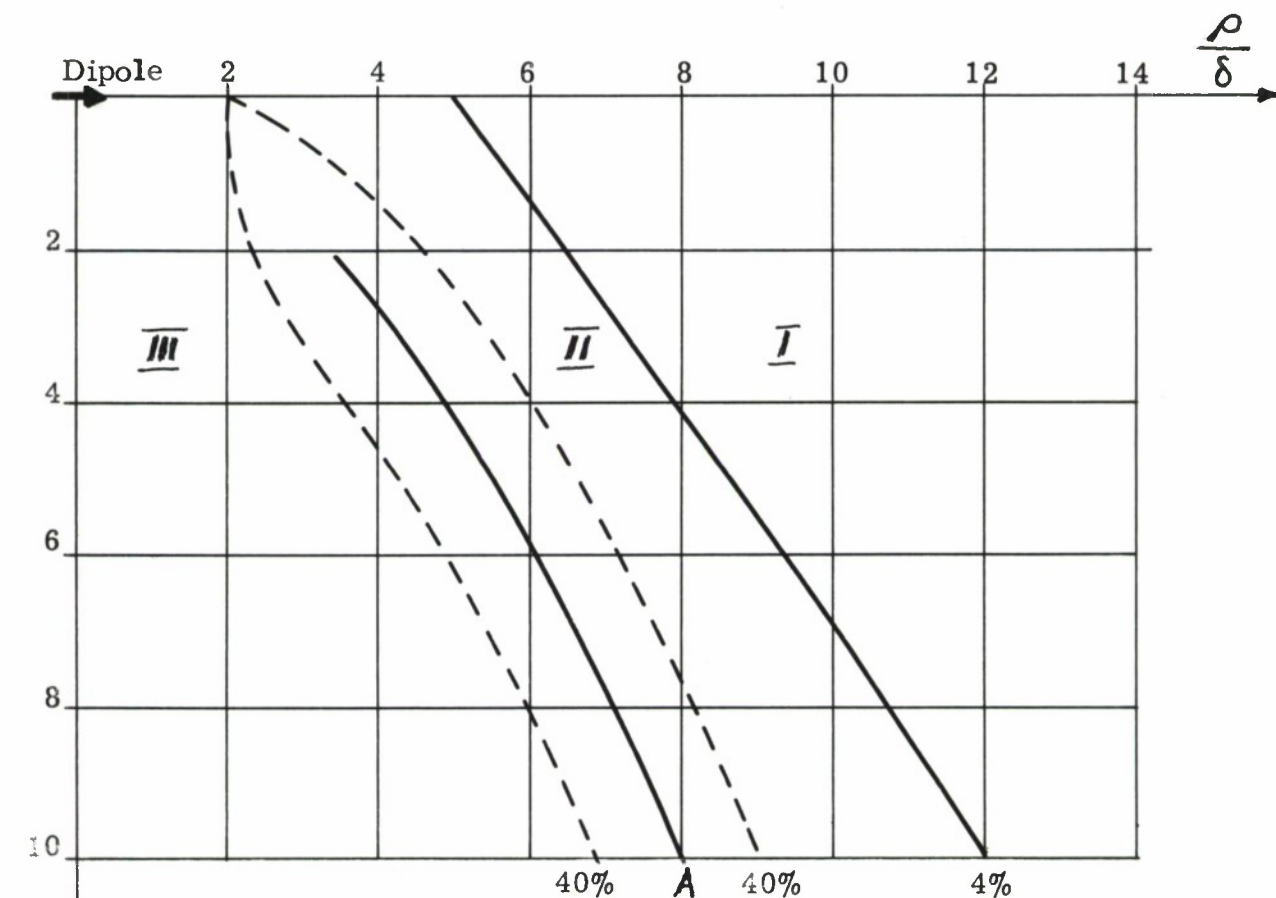


Fig. 12

Calculation of the field from a coaxial antenna in a conducting medium



$$\underline{I}: E_{1\rho} = \frac{Idl}{2\pi\sigma} \cdot \frac{e^{-\gamma z}}{\rho^3} \cos \varphi$$

\underline{II} : As in I. Error increasing towards dotted line

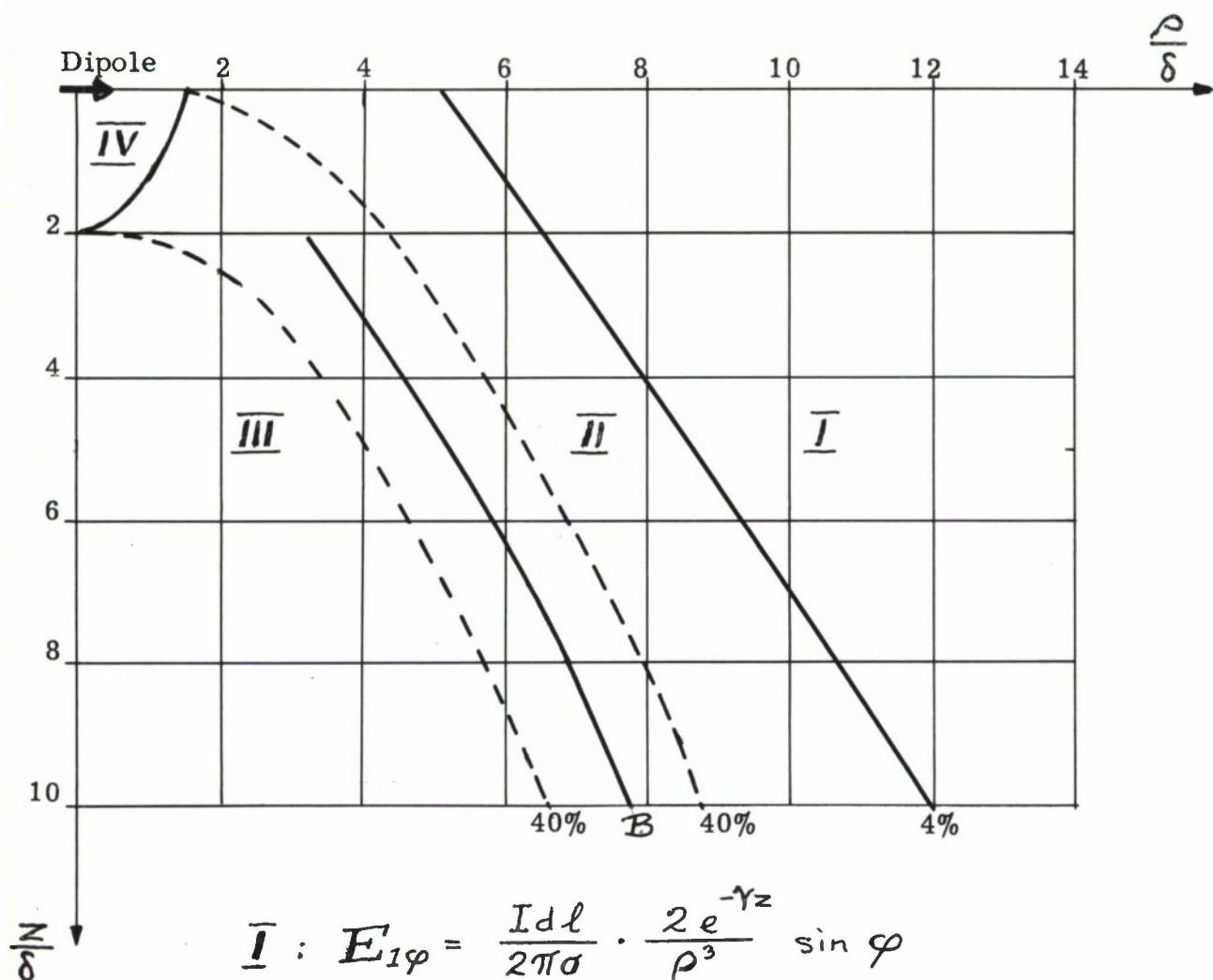
$$\underline{III}: E_{1\rho} = \frac{Idl}{2\pi\sigma} \cdot \frac{e^{-\gamma R}}{R^3} \left[\frac{\rho^2}{R^2} (3 + 3\gamma R + \gamma^2 R^2) - (1 + \gamma R + \gamma^2 R^2) \right] \cos \varphi$$

where $R = \sqrt{\rho^2 + z^2}$

Error decreasing for $R \rightarrow 0$, $\rho \rightarrow 0$, $z \rightarrow \infty$

Fig. 13

Estimate of errors in field expressions for $E_{1\rho}$ of dipole at the boundary



$$\underline{I} : E_{1\varphi} = \frac{Idl}{2\pi\sigma} \cdot \frac{2e^{-\gamma z}}{\rho^3} \sin \varphi$$

II : As in I. Error increasing towards dotted line

$$\underline{III} : E_{1\varphi} = \frac{Idl}{2\pi\sigma} \cdot \frac{\gamma z^2 \cdot e^{-\gamma R}}{R^3} \sin \varphi$$

Error decreasing for $\rho \rightarrow 0, z \rightarrow \infty$

$$\underline{IV} : E_{1\varphi} = \frac{Idl}{2\pi\sigma} \cdot \frac{e^{-\gamma R}}{R^3} (1 + \gamma R + \gamma^2 R^2) \sin \varphi$$

where $R = \sqrt{\rho^2 + z^2}$

Error decreasing for $R \rightarrow 0$

Fig. 14

Estimate of errors in field expressions for $E_{1\varphi}$ of dipole at the boundary

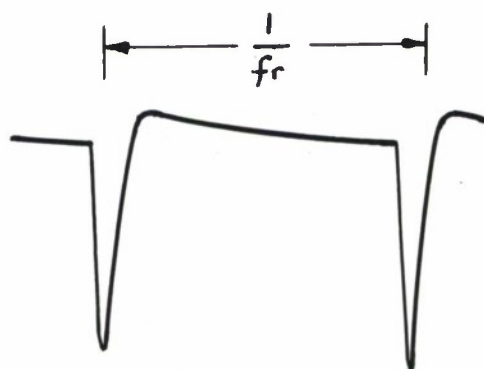


Fig. 15

Waveform of transmitter current

Peak value ~ 10 amp-m

$\rho_0 = 40 \text{ m}$ $\delta = 4 \text{ mho/m}$ $\theta = 10^\circ$
 \odot EXPERIMENTAL POINTS 10 cps
 \square EXPERIMENTAL POINTS 20 cps

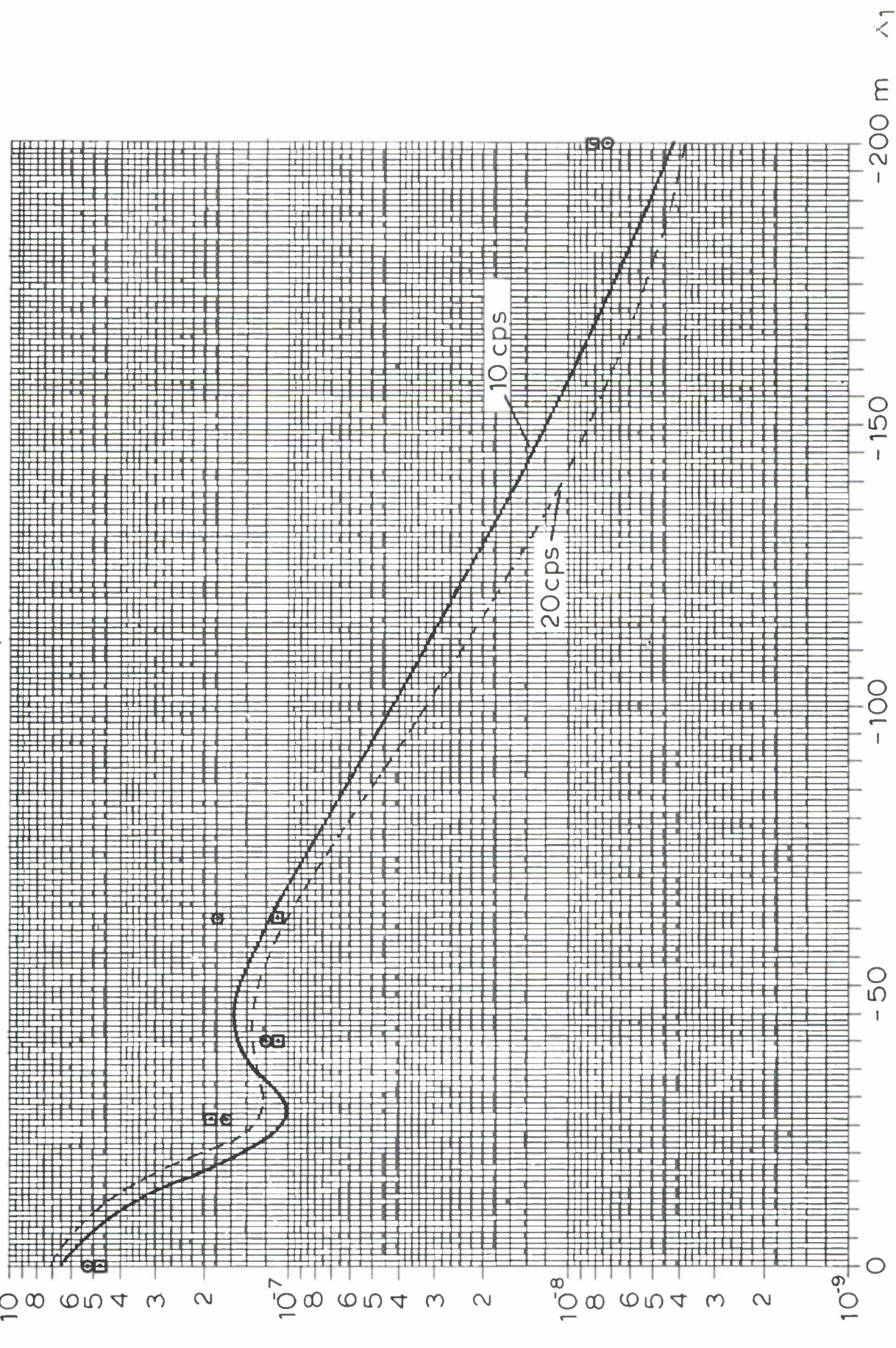


Fig. 16 Result of propagation experiment.

APPENDIX I

Computer programme for evaluating the modulus of the transfer-function in the range of $-200 \leq x_1 \leq 200$ m for various combinations of the frequency f , the distance of closest approach ρ_0 , the conductivity σ and the angle θ . (Written in "Algol" for an Elliott 503 computer):-

Transfer function, modulus of E/M , in very near field close to boundary of lossy half space. issue No. 2, L.B.-N., Nov. 1964;

begin real f , ρ_{00} , σ , θ , x_1 , t , u , v , P , Q , ρ , TF ; integer c ;
switch s : = next;

procedure $PQ(x, y, z, P, Q)$; value x, y, z ; real x, y, z, P, Q ;

begin real p, q, r ; $r := 0.0019869 * x * \text{sqrt}(y * z)$;

$p := \exp(-r) * \text{sqrt}(2 * r^2 + 2 * r + 1)$;

$q := \arctan(r / (1 + r)) - r$;

$P := p * \cos(q)$; $Q := p * \sin(q)$

end of procedure PQ ;

next: read f , ρ_{00} , σ , θ ; same line; print f f 15? f = ? , aligned (2, 1), f ,
 $\text{f cps } \rho_{00} = ?$, aligned (3, 1), ρ_{00} , $\text{f m } \sigma = ?$, aligned (1, 1), σ ,
 $\text{f S/m } \theta = ?$, aligned (2, 1), θ , f deg. ? ; print f f 1?? ;

$t := \theta * 0.0174533$; $u := \cos(t)$; $c := 0$; prefix (f f s3??); scaled (3);

for $x_1 := 200$ step 10.0 until 200.5 do

begin if $c - (c \text{ div } 5) * 5 = 0$ then print f f 1?? ;

$\rho := \text{sqrt}(x_1^2 + \rho_{00}^2)$; $v := \arctan(x_1 / \rho_{00})$;

$c := c + 1$; $PQ(\rho, f, \sigma, P, Q)$;

$TF := \text{sqrt}((2 * P * u - u - 3 * \cos(v - t))^2 + (2 * Q * u)^2) / \rho^3 /$
 $12.56637 / \sigma$;

print TF

end;

goto next

end of program transferfunction;

DISTRIBUTION LIST

Minister of Defense Brussels, Belgium	10 copies	Commander in Chief Western Atlantic Area (CINCWESTLANT) Norfolk 23511, Virginia	1 copy
Minister of National Defense Department of National Defense Ottawa, Canada	10 copies	Commander in Chief Eastern Atlantic Area (CINCEASTLANT) Eastbury Park, Northwood Middlesex, England	1 copy
Chief of Defense, Denmark Kastellet Copenhagen Ø, Denmark	10 copies	Maritime Air Commander Eastern Atlantic Area (COMAIREASTLANT) R. A. F. Northwood Middlesex, England	1 copy
Minister of National Defense Division Transmissions-Ecoute-Radar 51 Latour Maubourg Paris 7 ^e , France	10 copies	Commander Submarine Force Eastern Atlantic (COMSUBEASTLANT) Fort Blockhouse Gosport, Hants, England	1 copy
Minister of Defense Federal Republic of Germany Bonn, Germany	10 copies	Commander, Canadian Atlantic (COMCANLANT) H. M. C. Dockyard Halifax, Nova Scotia	1 copy
Minister of Defense Athens, Greece	10 copies	Commander Ocean Sub-Area (COMOCEANLANT) Norfolk 23511, Virginia	1 copy
Ministero della Difesa Stato Maggiore Marina Roma, Italy	10 copies	Supreme Allied Commander Europe (SACEUR) Paris, France	7 copies
Minister of National Defense Plein 4, The Hague, Netherlands	10 copies	SHAPE Technical Center P.O. Box 174 Stadhouders Plantsoen 15 The Hague, Netherlands	1 copy
Minister of National Defense Storgaten 33, Oslo, Norway	10 copies	Allied Commander in Chief Channel (CINCCHAN) Fort Southwick, Fareham Hampshire, England	1 copy
Minister of National Defense Lisboa, Portugal	10 copies	Commander Allied Maritime Air Force Channel (COMAIRCHAN) Northwood, England	1 copy
Minister of National Defense Ankara, Turkey	10 copies	Commander in Chief Allied Forces Mediterranean (CINCAFMED) Malta, G. C.	1 copy
Minister of Defense London, England	20 copies	Commander South East Mediterranean (COMEDSOU EAST) Malta, G. C.	1 copy
Supreme Allied Commander Atlantic (SACLANT) Norfolk 23511, Virginia	3 copies		
SACLANT Representative in Europe (SACLANTREPEUR) Place du Marechal de Lattre de Tassigny Paris 16 ^e , France	1 copy		

Commander Central Mediterranean (COMEDCENT) Naples, Italy	1 copy	NLR Netherlands Netherlands Joint Staff Mission 4200 Linneau Avenue Washington, D.C. 20008	1 copy
Commander Submarine Allied Command Atlantic (COMSUBACLANT) Norfolk 23511, Virginia	1 copy	NLR Norway Norwegian Military Mission 2720 34th Street, N.W. Washington, D.C.	1 copy
Commander Submarine Mediterranean (COMSUBMED) Malta, G.C.	1 copy	NLR Portugal Portuguese Military Mission 2310 Tracy Place, N.W. Washington, D.C.	1 copy
Standing Group, NATO (SGN) Room 2C256, The Pentagon Washington 25, D.C.	3 copies	NLR Turkey Turkish Joint Staff Mission 2125 LeRoy Place, N.W. Washington, D.C.	1 copy
Standing Group Representative (SGREP) Place du Marechal de Lattre de Tassigny Paris 16 ^e , France	5 copies	NLR United Kingdom British Defence Staffs, Washington 3100 Massachusetts Avenue, N.W. Washington, D.C.	1 copy
ASG for Scientific Affairs NATO Porte Dauphine Paris 16 ^e , France	1 copy	NLR United States SACLANT Norfolk 23511, Virginia	40 copies
<u>National Liaison Representatives</u>			
NLR Belgium Belgian Military Mission 3330 Garfield Street, N.W. Washington, D.C.	1 copy	<u>Scientific Committee of National Representatives</u>	
NLR Canada Canadian Joint Staff 2450 Massachusetts Avenue, N.W. Washington, D.C.	1 copy	Dr. W. Petrie Defence Research Board Department of National Defence Ottawa, Canada	1 copy
NLR Denmark Danish Military Mission 3200 Massachusetts Avenue, N.W. Washington, D.C.	1 copy	G. Meunier Ingenieur en Chef des Genie Maritime Services Technique des Constructions et Armes Navales 8 Boulevard Victor Paris 15 ^e , France	1 copy
NLR France French Military Mission 1759 "R" Street, N.W. Washington, D.C.	1 copy	Dr. E. Schulze Bundesministerium der Verteidigung ABT H ROMAN 2/3 Bonn, Germany	1 copy
NLR Germany German Military Mission 3215 Cathedral Avenue, N.W. Washington, D.C.	1 copy	Commander A. Pettas Ministry of National Defense Athens, Greece	1 copy
NLR Greece Greek Military Mission 2228 Massachusetts Avenue, N.W. Washington, D.C.	1 copy	Professor Dr. M. Federici Segreteria NATO MARIPERMAN La Spezia	1 copy
NLR Italy Italian Military Mission 3221 Garfield Street, N.W. Washington, D.C.	1 copy	Dr. M.W. Van Batenburg Fysisch Laboratorium RVO-TNO Walsdorpvlakte The Hague, Netherlands	1 copy

Mr. A.W. Ross
Director of Naval Physical Research
Ministry of Defence (Naval)
Bank Block
Old Admiralty Building
Whitehall, London S.W. 1

1 copy

Dr. J.E. Henderson
Applied Physics Laboratory
University of Washington
1013 Northeast 40th Street
Seattle 5, Washington

1 copy

Capitaine de Fregate R. C. Lambert
Etat Major Général Force Navale
Caserne Prince Baudouin
Place Dailly
Bruxelles, Belgique

1 copy

CAPT H. L. Prause
Søvaernets Televaesen
Lergravsvej 55
Copenhagen S', Denmark

1 copy

Mr. F. Lied
Norwegian Defense Research
Establishment
Kjeller, Norway

1 copy

Ing. CAPT N. Berkay
Seyir Ve HDR D
CUBUKLU
Istanbul, Turkey

1 copy

National Liaison Officers

Mr. Sv. F. Larsen
Danish Defense Research Board
Østerbrogades Kaserne
Copenhagen Ø, Denmark

1 copy

CDR R. J. M. Sabatier
EMM/TER
2 Rue Royale
Paris 8e, France

1 copy

Capitano di Fregata U. Gilli
Stato Maggiore della Marina
Roma, Italia

1 copy

LCDR J.W. Davis, USN
Office of Naval Research
Branch Office, London
Box 39, Fleet Post Office
New York, N.Y. 09510

1 copy

CDR Jose E.E.C. de Ataide
Instituto Hydrografico
Rua Do Arsenal Porta H-1
Lisboa 2, Portugal

1 copy